



## Synthetic approaches towards [<sup>18</sup>F]fluoro-DOG1, a potential radiotracer for the imaging of gastrointestinal stromal tumors



Martin Prause<sup>a</sup>, Sabrina Niedermoser<sup>a</sup>, Ralf Schirmmayer<sup>b</sup>, Carmen Wängler<sup>c</sup>, Björn Wängler<sup>a,\*</sup>

<sup>a</sup> Molecular Imaging and Radiochemistry, Department of Clinical Radiology and Nuclear Medicine, Medical Faculty Mannheim of Heidelberg University, Theodor-Kutzer-Ufer 1-3, 68167 Mannheim, Germany

<sup>b</sup> Department of Oncology, Division Oncological Imaging, University of Alberta, 11560 University Avenue, Edmonton, AB T6G 1Z2 Canada

<sup>c</sup> Biomedical Imaging, Department of Clinical Radiology and Nuclear Medicine, Medical Faculty Mannheim of Heidelberg University, Theodor-Kutzer-Ufer 1-3, 68167 Mannheim, Germany

### ARTICLE INFO

#### Article history:

Received 7 June 2018

Revised 17 July 2018

Accepted 20 July 2018

Available online 21 July 2018

#### Keywords:

DOG1

Gastrointestinal stromal tumors

Fluorine-18

Positron Emission Tomography (PET)

### ABSTRACT

Gastrointestinal stromal tumors (GIST) can currently only be identified by invasive biopsy sampling followed by immunohistochemical analysis. It would however be highly advantageous to have a radioligand able to bind the calcium-activated chloride channel DOG1, which is specific for GIST, and thus enable the sensitive, non-invasive and specific functional imaging of the disease by Positron Emission Tomography (PET). For this purpose, we developed different synthetic strategies towards a 4-phenylthiazole-2-amine-based labeling precursor that can be directly reacted with <sup>18</sup>F-fluoride to yield a radiotracer intended to bind DOG1. Of these, a boronic acid pinacol ester radiolabeling precursor could be efficiently reacted with <sup>18</sup>F in a one-step reaction, and the target radioligand [<sup>18</sup>F]fluoro-DOG1 be obtained in radiochemical yields of 34.0 ± 11.1% within 85 min overall synthesis time.

© 2018 Elsevier Ltd. All rights reserved.

### Introduction

Gastrointestinal stromal tumors (GIST) are the most common mesenchymal tumors [1], and most of them (85–95%) have primary mutations in the receptor tyrosine kinase KIT (also known as c-Kit or CD117) and PDGFRA (platelet-derived growth factor receptor alpha) leading to permanent activation of these kinases [2,3]. In 2002, the FDA approved the tyrosine kinase inhibitor Imatinib for the treatment of GIST, which prolonged the medium survival of patients suffering from metastatic GIST from 19 months without treatment to over 50 months with Imatinib treatment [4–8]. The high specificity of Imatinib towards KIT causes only minor side effects and results in good treatment results as long as no mutations occur [9–12]. GIST is commonly identified via biopsy sampling and subsequent immunohistochemical and/or genetic analysis. For immunohistochemical analysis, antibodies against KIT and CD34 are usually employed. However, antibodies against the calcium-activated chloride channel DOG1 (DOG: discovered on GIST) have proven to possess an even higher sensitivity

as well as specificity for the identification of GIST and are therefore of great interest for the sensitive and correct diagnosis of this disease, especially in those malignancies exhibiting no mutations in KIT [13–15].

DOG1 (also known as TMEM16A or ANO1) is expressed on epithelial tissue, including the interstitial cells of Cajal (ICC), which are supposed to be the origin of GIST [16–18]. It possesses pacemaker activity in ICCs and is therefore involved in the regulation of peristalsis in the gastrointestinal tract [19] as well as in regulating transepithelial water transport. This mechanism is also involved in the mucociliary clearance of the lungs, making DOG1 an interesting target for research on cystic fibrosis, asthma and other diseases as well [20–22]. In oncology, the ion channel DOG1 is used as a reliable biomarker in clinical routine for the distinction between GIST and other sarcoma due to its very high expression rate in 98% of all GIST biopsies [2,15,23].

Although DOG1-specific antibodies for immunohistochemistry exist and show high sensitivity and specificity for the target protein [13–15], they bind to an intracellular domain of the ion channel. This limits their usefulness as imaging agents in an *in vivo* imaging setting and results in the demand for an ideally small molecule radiotracer being able to address DOG1.

Such a radioligand would make burdensome biopsy sampling of GIST-suspect lesions dispensable as it would enable the correct diagnosis of the disease via non-invasive *in vivo* imaging with PET.

\* Corresponding author.

E-mail addresses: [Martin.Prause@medma.uni-heidelberg.de](mailto:Martin.Prause@medma.uni-heidelberg.de) (M. Prause), [Sabrina.Niedermoser@medma.uni-heidelberg.de](mailto:Sabrina.Niedermoser@medma.uni-heidelberg.de) (S. Niedermoser), [schirmma@ualberta.ca](mailto:schirmma@ualberta.ca) (R. Schirmmayer), [Carmen.Waengler@medma.uni-heidelberg.de](mailto:Carmen.Waengler@medma.uni-heidelberg.de) (C. Wängler), [Bjoern.Waengler@medma.uni-heidelberg.de](mailto:Bjoern.Waengler@medma.uni-heidelberg.de) (B. Wängler).

## Results and discussion

Thus, the aim of this work was to develop a  $^{18}\text{F}$ -labeled small molecule PET radiotracer intended to specifically bind to DOG1 and to allow the efficient *in vivo* visualization of GIST *via* PET.

For this purpose, a labeling precursor had to be developed which enables the efficient, ideally one-step introduction of  $^{18}\text{F}$  *via* nucleophilic substitution and thus provides an efficient synthesis of the target radiotracer.

As a biologically active scaffold for the target radioligand, a 4-phenylthiazole-2-amine core structure (Fig. 1) was chosen as Namkung and co-workers were able to show by high-throughput-screening of different compound classes that this substance class is best suited to give highly potent activators, as well as inhibitors, of DOG1 [21,22].

A particular challenge in developing a  $^{18}\text{F}$ -labeled 4-phenylthiazole-2-amine derivative was the position that the radiolabel had to be introduced into. The  $\text{R}^1$  position is – despite the unfavorably high electron density – the best opportunity for the introduction of [ $^{18}\text{F}$ ]fluoride. Previously it was shown that the introduction of a 4-fluorophenyl substituent in the  $\text{R}^1$  position is well tolerated with regard to the binding characteristics compared with the lead structure, whereas  $^{18}\text{F}$ -introduction in the  $\text{R}^3$  position resulted in a considerably decreased biological activity (Fig. 1A) [22].

In a first attempt, we synthesized a nitro precursor (see ESI for details) of the target substance (Fig. 1C) over two steps in good overall yield (64%). In the following radiosynthesis, no reaction of the precursor molecule with [ $^{18}\text{F}$ ]fluoride could be observed at lower temperatures of 80–100 °C. A possible explanation for this is the high electron density of the aromatic system the nitro leaving group is attached to which is caused by the 2-aminothiazole ring. Thus, harsher reaction conditions were necessary which resulted – despite the optimization of several reaction parameters such as solvent, temperature, base and precursor concentrations (see ESI for details) – in significant decomposition of the precursor before a considerable incorporation of [ $^{18}\text{F}$ ]fluoride could be achieved. As the precursor decomposition occurred faster than the incorporation of [ $^{18}\text{F}$ ]fluoride, no product could be isolated.

In a second attempt, we synthesized a triazene precursor (see ESI for details) since the  $^{18}\text{F}$ -radiolabeling of electron rich aromatic

compounds was shown to be feasible at mild reaction temperatures *via* triazenes [24–26], forming highly reactive diazonium ion intermediates *in situ* upon the addition of trifluoromethanesulfonic acid [27–29]. Although the labeling precursor could be obtained in four steps in moderate overall yield (19%), this approach also resulted in the formation of many by-products during  $^{18}\text{F}$ -labeling and no product formation could be observed using different labeling conditions (see ESI for details). Another difficulty using this type of reaction is that the optimization of reaction parameters is not easy since by-products can readily be formed with every compound in the reaction mixture, e.g. solvents [27,28], and considerable amounts of volatile [ $^{18}\text{F}$ ]HF are generated under the acidic reaction conditions, further decreasing the achievable radiochemical yields.

Thus, we finally decided to change the synthetic strategy to the copper-catalyzed radiofluorination of aryl boronic acid esters. This promising radiofluorination pathway is applicable to electron-poor as well as electron-rich precursor compounds and is known for its high selectivity and relatively mild reaction conditions for  $^{18}\text{F}$ -introduction [30,31].

The target boronic acid pinacol ester (BPin) precursor **3** was obtained within three steps in good overall yield (37%, Scheme 1). The synthesis started with the bromination of 4-acetylphenylboronic acid pinacol ester at the alpha position with *N*-bromosuccinimide. The  $\alpha$ -bromoketone **1** was obtained after column chromatography and subsequent recrystallization in good yield (67%). The  $^1\text{H}$  and  $^{13}\text{C}$  NMR spectra of the product showed keto-enol tautomerism and fast deuterium-hydrogen exchange and confirmed the identity of **1**.  $\alpha$ -Bromoketone **1** was then reacted with *N*-benzylthiourea in a Hantzsch' thiazole synthesis, giving 2-aminothiazole **2** in high yield (79%). The last step of the boronic acid pinacol ester precursor synthesis was the formation of the amide bond by condensation of 2-aminothiazole **2** and 3,4,5-trimethoxybenzoyl chloride, giving the radiolabeling precursor BPin-DOG1 (**3**) in good yield (70%) and excellent purity (>97%). Noteworthy is that the boronic acid ester formed a reversible, pH-dependent equilibrium with the respective borate complex in aqueous solution which was observable by analytical HPLC and is in accordance with earlier observations [32]. The non-radioactive reference compound [ $^{19}\text{F}$ ]fluoro-DOG1 (**5**) was obtained in an

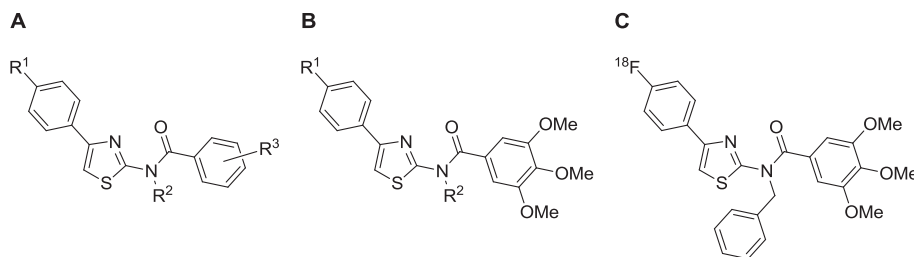
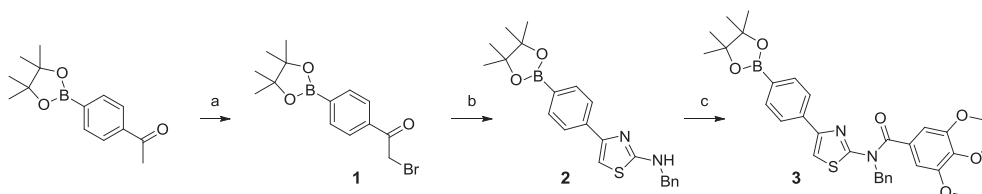
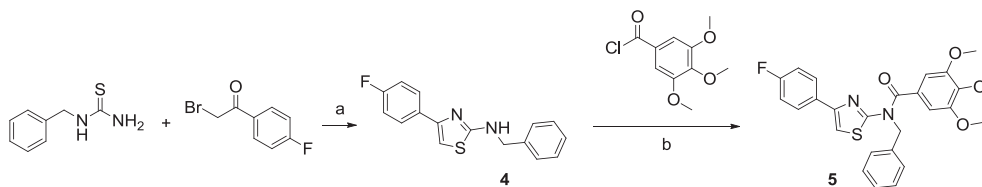


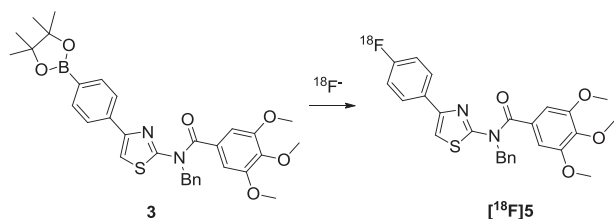
**Figure 1.** General structure of DOG1 activators based on the 4-phenylthiazole-2-amine scaffold (A), structural lead showing high potency in terms of DOG1 binding (B) and the target  $^{18}\text{F}$ -labeled DOG1 radioligand (C).



**Scheme 1.** Schematic depiction of the reaction pathway towards the radiolabeling precursor boronic acid pinacol ester (DOG1-BPin, **3**). Reagents and conditions: (a) *N*-bromosuccinimide (1.1 eq., 5.5 mmol), *p*-toluene sulfonic acid (1.1 eq., 5.5 mmol), MeCN (50 mL), 50 °C, 3 h (67%); (b) *N*-benzylthiourea (1.0 eq., 2.3 mmol), MeCN (6 mL + 0.017% TFA), 80 °C, 2 h (79%); (c) 3,4,5-trimethoxybenzoyl chloride (2.0 eq., 2.8 mmol), pyridine (8.0 eq., 11.3 mmol), toluene (10 mL), 110 °C, 8 h (70%).



**Scheme 2.** Schematic depiction of the reaction pathway towards the cold reference compound F-DOG1 (**5**). Reagents and conditions: (a) 2-Bromo-1-(4-fluorophenyl)ethan-1-one (2 mmol), *N*-benzylthiourea (1.0 eq., 2 mmol), EtOH (8 mL), 80 °C, 30 min (quant.); (b) 3,4,5-trimethoxybenzoyl chloride (4 eq., 1 mmol), pyridine (8 eq., 2 mmol), toluene (5 mL), 110 °C, 5 h (89%).



**Scheme 3.** Schematic depiction of the radiosynthesis of  $^{18}\text{F}$ -DOG1 ( $^{18}\text{F}$ **5**). Reagents and conditions: **3** (11.7 mg, 20  $\mu\text{mol}$ ),  $^{18}\text{F}$ ]/KF/K2.2.2 (16.7  $\mu\text{mol}$ ),  $\text{K}_2\text{C}_2\text{O}_4$  (6.02  $\mu\text{mol}$ ),  $\text{K}_2\text{CO}_3$  (0.76  $\mu\text{mol}$ ),  $[\text{Cu}(\text{OTf})_2(\text{py})_4]$  (13.6 mg, 20  $\mu\text{mol}$ ), DMA (400  $\mu\text{L}$ ), 120 °C, 20 min, RCY: 34.0  $\pm$  11.1%.

excellent overall yield (89%) over two steps via Hantzsch' thiazole synthesis, first reacting 2-bromo-1-(4-fluorophenyl)ethan-1-one and *N*-benzylthiourea followed by the condensation of intermediate (**4**) with 3,4,5-trimethoxybenzoyl chloride analogously to the reaction pathway to the BPin precursor **3** (see ESI for details) (Scheme 2).

The radiofluorination of **3** (Scheme 3) to product  $^{18}\text{F}$ **5** was performed according to the protocol described by Preshlock and co-workers for electron-rich compounds [30].

$^{18}\text{F}$ fluoride was eluted from the QMA cartridge using an optimized  $^{18}\text{F}$ -elution cocktail consisting of K2.2.2, potassium carbonate and potassium oxalate in MeCN : H<sub>2</sub>O (8 : 2, v/v, 1 mL).

Noteworthy, higher amounts of potassium carbonate resulted in degradation of the copper catalyst during the reaction.

For the  $^{18}\text{F}$ -introduction, equimolar amounts of the catalyst tetrakis(pyridine)copper(II) triflate (20  $\mu\text{mol}$ ) and the BPin precursor **3** (20  $\mu\text{mol}$ ) were found to be ideal since the catalyst is subject to decomposition processes under the radiolabeling conditions applied. As described by Preshlock and co-workers [27], the solvent plays an important role for this reaction type, an observation which we were able to confirm. For example, using DMF, a  $^{18}\text{F}$  fluoride incorporation of only 36% could be achieved, whereas in DMA, an incorporation rate of 74  $\pm$  8% (n = 10) was found under otherwise identical reaction conditions.

The product  $^{18}\text{F}$ **5** was purified via semipreparative radio-HPLC, trapped on a C18 cartridge and eluted with 90% ethanol (containing 0.125 mg/mL ascorbic acid as stabilizing agent). The ethanolic product solution was diluted with saline to a final EtOH concentration of <10% (v/v) and the product was obtained in excellent radiochemical purity (Fig. 2), radiochemical yields of 34.0  $\pm$  11.1% and molar activities of 8.2  $\pm$  3.0 GBq/ $\mu\text{mol}$  at the end of synthesis within 85 min (n = 7).

Thus, although all three reaction pathways towards  $^{18}\text{F}$ **5** should be able to generate the product by nucleophilic substitution,  $^{18}\text{F}$ **5** could only be obtained using the BPin precursor approach.

Although the radiosynthesis of  $^{18}\text{F}$ **5** proceeded efficiently under the optimized conditions using the BPin precursor, giving the product in good RCYs, the achieved molar activity (determined

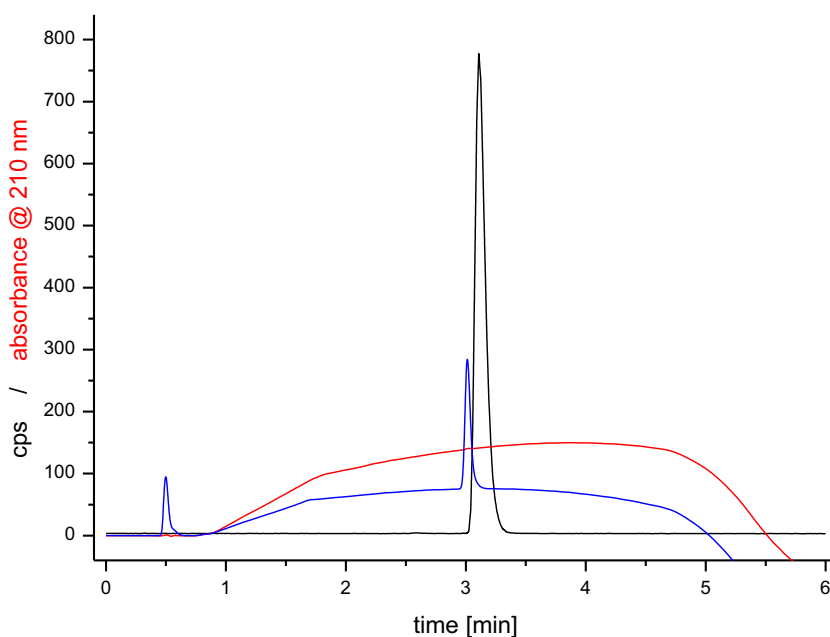


**Figure 2.** Analytical radio-HPLC chromatograms of the purified radiotracer  $^{18}\text{F}$ **5** and of the reference compound **5**. Black: radioactive signal of  $^{18}\text{F}$ **5**, red: corresponding UV signal of  $^{18}\text{F}$ **5** at 210 nm, blue: UV signal of reference compound **5** at 210 nm. Gradient: 0–1 min: 0–30% MeCN, 1–4 min: 30–70% MeCN, 4–5 min: 70–100% MeCN, 5–6 min: 100% MeCN.

by analytical radio-HPLC by the area of the obtained UV signal of the carrier of [ $^{18}\text{F}$ ]5 at 214 nm wavelength and a standard curve of 5) was rather low. As the semipreparative radio-HPLC purification of the product proceeded well, we have no explanation for this phenomenon.

Next, the stability and lipophilicity of [ $^{18}\text{F}$ ]5 were evaluated. [ $^{18}\text{F}$ ]5 was demonstrated to be stable in a phosphate buffered solution (1 mM, pH 7.0–7.4) for 2 h at ambient temperature. In terms of lipophilicity/hydrophilicity, the distribution coefficient  $\log_D$  (evaluated in 1-octanol/phosphate buffer (0.05 M, pH 7.4)) was determined to be  $2.51 \pm 0.13$  ( $n = 6$ ). In addition to the stability test performed in the phosphate buffered solution, we also evaluated the stability of the radioligand in blood sera of different origin. In human serum, the radiotracer showed excellent stability (>99%) after 2 h at 37 °C. In contrast, [ $^{18}\text{F}$ ]5 decomposed rather quickly in murine and rat serum, resulting in only 16.5% and 3.4% intact tracer after 2 h at 37 °C, respectively (Fig. S1). Due to the high stability of the radiotracer in human serum, [ $^{18}\text{F}$ ]5 could nevertheless be interesting for human GIST imaging. The next steps for *in vitro* evaluation of the potential of the newly developed radiotracer for human application in PET imaging could involve molecular modeling of the interaction of [ $^{18}\text{F}$ ]5 with DOG1 as well as evaluation of the binding specificity of the radioligand to the target protein.

## Conclusion

Herein, we report the first example of a  $^{18}\text{F}$ -labeled small molecule radiotracer intended for the non-invasive PET imaging of DOG1. This included the organic syntheses of different radiolabeling precursors as well as the development and optimization of the corresponding  $^{18}\text{F}$ -radiosyntheses.

Among the developed and tested approaches (using a nitro, a triazene and an aryl boronic acid ester as precursors for subsequent  $^{18}\text{F}$ -radiolabeling), only the aryl boronic acid ester precursor enabled the efficient one-step incorporation of  $^{18}\text{F}$ , thus demonstrating the superiority of this pathway for nucleophilic  $^{18}\text{F}$ -radiolabeling of electron-rich precursor molecules over other, more common approaches.

## Acknowledgements

This work was supported by the European Community's 7th Framework Programme [FP7/2007–2013; grant agreement number 602306] and the German Federal Ministry of Education and Research (BMBF) [funding code number 13GW0091E]. Further, the authors thank Dr. W. Spahl (LMU, Munich) for ESI mass spectrometry measurements.

## A. Supplementary data

Supplementary data associated with this article can be found, in the online version, at <https://doi.org/10.1016/j.tetlet.2018.07.050>.

## References

- [1] A.W. Beham, I.-M. Schaefer, P. Schüler, S. Cameron, Ghadimi B. Michael, *Int. J. Colorectal Dis.* 27 (2011) 689–700.
- [2] Z.A. Kamar, A.A.F. Sedky, O.H. Nada, N.M. Abd Raboh, N.M. El-Mishad, *Egypt. J. Pathol.* 34 (2014) 89–95.
- [3] M. Linch, J. Claus, C. Benson, *OncoTargets Ther.* 6 (2013) 1011–1023.
- [4] C.D. Blanke, G.D. Demetri, M. von Mehren, M.C. Heinrich, B. Eisenberg, J.A. Fletcher, C.L. Corless, C.D.M. Fletcher, P.J. Roberts, D. Heinz, E. Wehre, Z. Nikolova, H. Joensuu, *J. Clin. Oncol.* 26 (2008) 620–625.
- [5] C.D. Blanke, C. Rankin, G.D. Demetri, C.W. Ryan, M. von Mehren, R.S. Benjamin, A.K. Raymond, V.H.C. Bramwell, L.H. Baker, R.G. Maki, M. Tanaka, J.R. Hecht, M. C. Heinrich, C.D.M. Fletcher, J.J. Crowley, E.C. Borden, *J. Clin. Oncol.* 26 (2008) 626–632.
- [6] J. Call, C.D. Walentas, J.C. Eickhoff, N. Scherzer, *BMC Cancer* (2012) 12.
- [7] U. De Giorgi, J. Verweij, *Mol. Cancer Ther.* 4 (2005) 495–501.
- [8] J.S. Gold, S.M. van der Zwan, M. Gonen, R.G. Maki, S. Singer, M.F. Brennan, C.R. Antonescu, R.P. De Matteo, *Ann. Surg. Oncol.* 14 (2007) 134–142.
- [9] C.R. Antonescu, P. Besmer, T.H. Guo, K. Arkun, G. Hom, B. Koryotowski, M.A. Leversha, P.D. Jeffrey, D. Desantis, S. Singer, M.F. Brennan, R.G. Maki, R.P. DeMatteo, *Clin. Cancer Res.* 11 (2005) 4182–4190.
- [10] M. Debiec-Rychter, J. Cools, H. Dumez, R. Sciot, M. Stul, N. Mentens, H. Vranckx, B. Wasag, H. Prenen, J. Roesel, A. Hagemeijer, A. Van Oosterom, P. Marynen, *Gastroenterology* 128 (2005) 270–279.
- [11] A.W. Gramza, C.L. Corless, M.C. Heinrich, *Clin. Cancer Res.* 15 (2009) 7510–7518.
- [12] J. Verweij, P.G. Casali, J. Zalcberg, A. LeCesne, P. Reichardt, J.Y. Blay, R. Issels, A. van Oosterom, P.C.W. Hogendoorn, M. Van Glabbeke, R. Bertulli, I. Judson, *Grp ESTBS, Grp IS, A.G. Tria, Lancet* 364 (2004) 1127–1134.
- [13] I. Espinosa, C.-H. Lee, M.K. Kim, B.-T. Rouse, S. Subramanian, K. Montgomery, S. Varma, C.L. Corless, M.C. Heinrich, K.S. Smith, Z. Wang, B. Rubin, T.O. Nielsen, R. S. Seitz, D.T. Ross, R.B. West, M.L. Cleary, M. van de Rijn, *Am. J. Surg. Pathol.* 32 (2008) 210–218.
- [14] B. Liegl, J.L. Hornick, C.L. Corless, C.D.M. Fletcher, *Am. J. Surg. Pathol.* 33 (2009) 437–446.
- [15] R.B. West, C.L. Corless, X. Chen, B.P. Rubin, S. Subramanian, K. Montgomery, S. Zhu, C.A. Ball, T.O. Nielsen, R. Patel, J.R. Goldblum, P.O. Brown, M.C. Heinrich, M. van de Rijn, *Am. J. Pathol.* 165 (2004) 107–113.
- [16] S.J. Hwang, P.J.A. Blair, F.C. Britton, K.E. O'Driscoll, G. Hennig, Y.R. Bayguinov, J. R. Rock, B.D. Harfe, K.M. Sanders, S.M. Ward, *J. Physiol.* 587 (2009) 4887–4904.
- [17] B. Manoury, A. Tamuleviciute, P. Tamaro, *J. Physiol.* 588 (2010) 2305–2314.
- [18] Y.D. Yang, H. Cho, J.Y. Koo, M.H. Tak, Y. Cho, W.-S. Shim, S.P. Park, J. Lee, B. Lee, B.-M. Kim, R. Raouf, Y.K. Shin, U. Oh, *Nature* 455 (2008) 1210–1215.
- [19] K.M. Sanders, M.H. Zhu, F. Britton, S.D. Koh, S.M. Ward, *Exp. Physiol.* 97 (2012) 200–206.
- [20] R. Tarran, B. Button, R.C. Boucher, *Ann. Rev. Physiol.* 68 (2006) 543–561.
- [21] W. Namkung, P.W. Phuan, A.S. Verkman, *J. Biol. Chem.* 286 (2011) 2365–2374.
- [22] W. Namkung, Z. Yao, W.E. Finkbeiner, A.S. Verkman, *FASEB J.* 25 (2011) 4048–4062.
- [23] S. Simon, F. Grabellus, L. Ferrera, L. Galiotta, B. Schwindenhammer, T. Muhlenberg, G. Taeger, G. Eilers, J. Treckmann, F. Breitenbuecher, M. Schuler, T. Taguchi, J.A. Fletcher, S. Bauer, *Cancer Res.* 73 (2013) 3661–3670.
- [24] T.J. Tewson, M.J. Welch, *ChemComm* (1979) 1149–1150.
- [25] J.S. Ng, J.A. Katzenellenbogen, M.R. Kilbourn, *J. Org. Chem.* 46 (1981) 2520–2528.
- [26] M.N. Rosenfeld, D.A. Widdowson, *ChemComm* (1979) 914–916.
- [27] T. Pages, B.R. Langlois, *J. Fluorine Chem.* 107 (2001) 321–327.
- [28] T. Pages, B.R. Langlois, D. Le Bars, P. Landais, *J. Fluorine Chem.* 107 (2001) 329–335.
- [29] P.J. Riss, S. Kuschel, F.I. Aigbirhio, *Tet. Lett.* 53 (2012) 1717–1719.
- [30] S. Preshlock, S. Calderwood, S. Verhoog, M. Tredwell, M. Huiban, A. Hienzsch, S. Gruber, T.C. Wilson, N.J. Taylor, T. Cailly, M. Schedler, T.L. Collier, J. Passchier, R. Smits, J. Mollitor, A. Hoepfing, M. Mueller, C. Genicot, J. Mercier, V. Gouverneur, *ChemComm* 52 (2016) 8361–8364.
- [31] M. Tredwell, S.M. Preshlock, N.J. Taylor, S. Gruber, M. Huiban, J. Passchier, J. Mercier, C. Genicot, V. Gouverneur, *Angew. Chem. Int. Edit.* 53 (2014) 7751–7755.
- [32] B.P. Carrow, J.F. Hartwig, *J. Am. Chem. Soc.* 133 (2011) 2116–2119.